

Electronic structure and optical properties of layered dichalcogenides: TiS_2 and TiSe_2 [†]

H. W. Myron

Magnetic Theory Group, Physics Department, Northwestern University, Evanston, Illinois 60201

A. J. Freeman

Physics Department, Northwestern University, Evanston, Illinois 60201

Argonne National Laboratory, Argonne, Illinois 60439

(Received 23 July 1973)

The electronic-energy-band structure of the layered dichalcogenides TiS_2 and TiSe_2 has been determined using the Korringa-Kohn-Rostoker (KKR) method. Crystal potentials were constructed from overlapping atomic charge densities in the muffin-tin approximation for both full Slater exchange and Kohn-Sham-Gaspár exchange and several different starting atomic configurations. Detailed results are given here for the potential based on the atomic configuration $3d^2 4s^2$ on the titanium atoms, $3p^4$ on the sulfur atoms, and $4p^4$ on the selenium atoms and with full Slater exchange. An energy gap of 2.0–2.7 eV between the occupied $3p$ sulfur bands and the empty $3d$ titanium bands is found for all potentials studied thereby confirming the traditional view of TiS_2 as a semiconductor. TiSe_2 is also found to be a semiconductor with a direct energy-band gap of 1.2 eV. The joint density of states calculated from the energy bands of these *ab initio* calculations are found to agree quite well with recently measured transmission spectra.

INTRODUCTION

The layered transition-metal dichalcogenides have become the subject of renewed experimental and theoretical interest because of their anisotropic optical and transport properties¹ and because of their possible importance as high-temperature superconductors. These MX_2 compounds, where M is a transition metal and X is a chalcogen (S, Se, Te), show a wide variety of electronic properties ranging from semiconducting (ZrS_2) to superconducting (PdTe_2). In the transition-metal layered compounds MX_2 , slabs are three atoms thick with the top and bottom layers of the slab formed from chalcogen atoms and the middle layer from the transition-metal atoms. The exact arrangement of the atoms within these layers varies from compound to compound, grouping them into two general categories: undistorted and distorted structures.^{1,2}

In these layered compounds the metal-to-metal interactions between layers are weak and the compounds have a pseudo-two-dimensional network of metal atoms. Work has been done³ on these compounds intercalated with organic molecules but these do not yield high T_c 's. Instead Barz *et al.*⁴ have found that where a structure containing a true three-dimensional network of metal atoms is synthesized from similar elements, tending to the M_3X_4 structure, the transition temperatures are much higher; namely, 10–13 K for $\text{Li}_x\text{Ti}_{1-x}\text{S}_2$ ($0.1 \leq x \leq 0.3$). An attempt⁵ to explain the superconducting properties of the $\text{Li}_x\text{Ti}_{1-x}\text{S}_2$ complex assumes that stoichiometric TiS_2 has a 1-eV gap between the titanium $3d$ and sulfur $3p$ valence bands and the Ti $4s$ conduction band. According to this model, excess Ti atoms would have their d states

fall in this 1-eV gap. Phillips presents several phenomenological arguments, based on McMillan's⁶ theory and the possible role of high $dN(E_F)/dE$ values, to explain why intercalating $\text{Ti}_{1-x}\text{S}_2$ with Li would increase the superconducting transition temperature.

Considerable experimental work has been completed recently in an attempt to understand stoichiometric TiS_2 via the optical,⁷ x-ray,⁸ and transport properties⁹ of this crystal. Whereas TiS_2 has been traditionally thought of as a semiconductor with a 1-eV gap, a view supported by recent optical data,⁷ both recent x-ray⁸ and transport-property work,⁹ are in apparent disagreement with this model.

This paper reports results of our study of the energy bands of TiS_2 and TiSe_2 using the Korringa-Kohn-Rostoker (KKR) or Green's-function method¹⁰ in the muffin-tin approximation. The results of these calculations agree favorably with the transmission spectra⁷ of TiS_2 and TiSe_2 and support the traditional view that these compounds are semiconductors. Comparisons of these results with the discrete-variational-method results of Ellis and Seth¹¹ for TiS_2 obtained at the high-symmetry points and the semiempirical results of Murray and Yoffe¹² show general agreement.

CALCULATION

TiS_2 has the layered CdI_2 structure, (1T phase) as shown in Fig. 1. Planes of titanium atoms are surrounded by planes of sulfur atoms, forming a sandwich structure, from above and below. The planes of sulfur atoms are located at $z = \pm \frac{1}{4}c$. The unit cells are arranged so that the metal atoms are stacked directly above each other. Within a unit

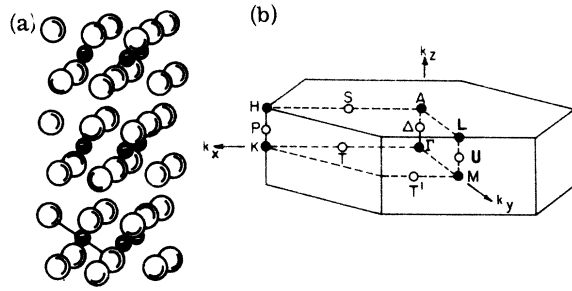


FIG. 1. (a) CdI_2 structure. The black circles are the metal atoms and the light circles are the chalcogen atoms. (b) Brillouin zone of the hexagonal Bravais lattice.

cell the sulfur atoms are arranged in octahedral coordination about the titanium atom.

The crystal potential is constructed along the usual lines¹³ for both full Slater ($\alpha = 1$) exchange¹⁴ and Kohn-Sham-Gaspár ($\alpha = \frac{2}{3}$) exchange¹⁵ using the Hartree-Fock-Slater atomic charge densities of Herman and Skillman. The neutral atomic charge densities are $3d^2 4s^2$ on Ti atoms and p^4 on the anions. The muffin-tin radii were chosen in order to maximize the total electronic charge within the muffin-tin spheres with the constraint that the sum of the muffin-tin radii is equal to the nearest neighbor distance. The lattice parameters are $a = 6.436$ a. u., $c = 10.756$ a. u. and $a = 6.684$ a. u., $c = 11.347$ a. u.,⁴ respectively, for TiS_2 and TiSe_2 ; the muffin-tin radii of TiS_2 are 1.9286 and 2.6362 a. u. and of TiSe_2 , 1.8693 and 2.8953 a. u. for the titanium and chalcogenide atoms, respectively.

In order to determine the stationary eigenvalues $E(\vec{k})$ one must solve the energy determinant^{10,16,17}

$$\det |\bar{M}| = \det |A_{\ell m; \ell' m'}^{(j, j')} + \delta_{j j'} \delta_{\ell \ell'} \delta_{m m'} \kappa \cot \eta_{\ell}| = 0, \quad (1)$$

where

$$\kappa = \begin{cases} \sqrt{E} & \text{for } E > 0 \\ i\sqrt{E} & \text{for } E < 0 \end{cases}$$

$A_{\ell m; \ell' m'}^{(j, j')}$ are the structure factors, E is the energy relative to the muffin-tin zero and η_{ℓ} is the partial-wave scattering phase shift. In setting up the energy matrix of the KKR method we have included states up to $\ell = 2$ for both titanium and sulfur so the order of the matrix is 27. The lattice and reciprocal sums in the structure factor converge well for 35 and 36 vectors, respectively, for a choice of the Ewald parameter¹⁶ of $\eta = (\pi/a)^2$. The usual way of determining the stationary eigenvalues is to fix \vec{k} and vary E on a fine grid until $\det |\bar{M}| = 0$. When the energy matrix is diagonalized, the determinant is the product of the eigenvalue spectrum. If any roots are in a certain energy increment the correction necessary to give a zero

eigenvalue is predicted by¹⁸

$$\delta E = -\lambda^{(i)}(E) / \left(\frac{\partial \lambda^{(i)}}{\partial E} \right). \quad (2)$$

Since the eigenvalue spectrum $\lambda^{(i)}$ is quite linear in the vicinity of a root, $\partial \lambda^{(i)} / \partial E$ is represented well by a straight-line fit. This procedure is continued until a predetermined tolerance (0.001 Ry) is achieved. Using this procedure the eigenvalues are determined within two or three iterations for a scanning energy of 0.04 to 0.05 Ry.

RESULTS

The energy bands of TiS_2 along the high-symmetry axes for full exchange ($\alpha = 1$) are shown in Fig. 2(a). The six lower-lying bands are primarily p -like from the sulfur and the five higher bands are d -like from the titanium atoms. The energy gap at Γ , 0.145 Ry, increases to 0.198 Ry for decreasing $\alpha (= \frac{2}{3})$, as has already been noted.¹¹ A recent determination¹² of the band structure of titanium disulfide using a semiempirical tight-binding band model gives an energy gap of 0.07 Ry. That this gap is smaller than that of the *ab initio* calculations is not surprising since the value of the band parameters has been adjusted to reproduce the traditional band gap of ~ 1 eV. The poor agreement between *ab initio* calculations and experimental determinations of the band gap is related to the fact that whereas the *ab initio* calculations are for the ground state of the system, the optical excitation corresponds to the creation of a hole in the valence band.

The over-all band picture of the three methods is quite similar. However, the semiempirical band model¹² has no band crossings and has different ordering of the eigenvalues at the high-symmetry points. For example, at Γ the results of the present work has the order of Γ_2^- and Γ_3^- and Γ_3^+ and Γ_1^+ interchanged with the work of Ref. 12. It is useful to compare d bandwidths, d - p gap, and p bandwidth of the two previous calculations with the result of this work at Γ (Table I). The d bandwidth of this calculation and Ref. 12 are the same and smaller than the width of Ref. 11. The p - d gap of this work and Ref. 11 agree quite well with each other but are almost twice as large as the semiempirical model where the band gap has been adjusted to the traditional band gap of ~ 1 eV. The p bandwidth of Ref. 12 is smaller than the value of this work and that of Ref. 11. This is not surprising since the model used in Ref. 12 is tight binding and the p band is not well localized. All calculations agree that the $4s$ conduction band is well above the $3d$ conduction band, which contradicts the microscopic model⁵ of superconductivity in bridge and layered compounds.

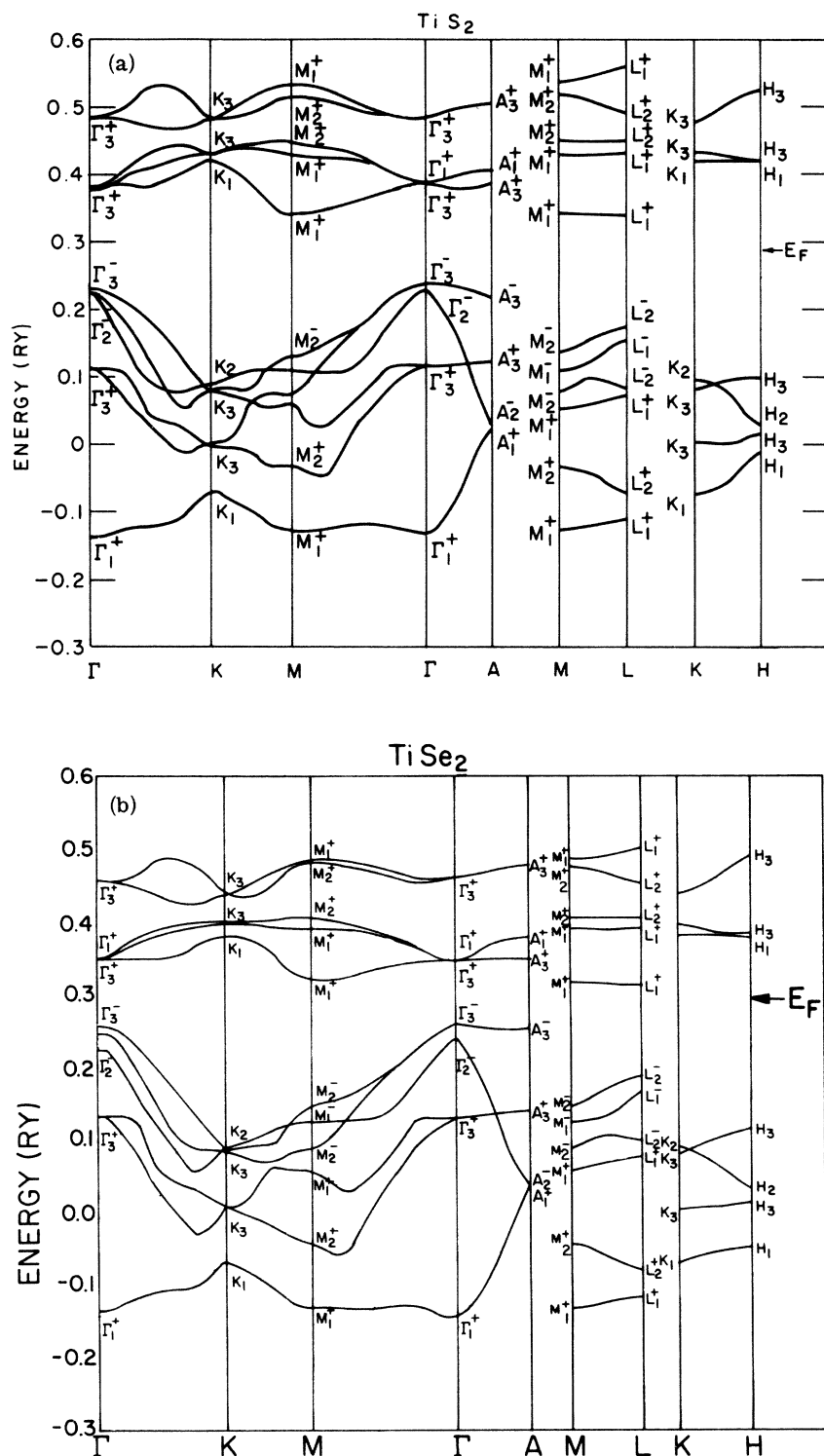


FIG. 2. (a) p and d bands of TiS_2 along some high-symmetry directions. (b) p and d bands of TiSe_2 along some high-symmetry direction.

The energy bands of TiSe_2 for full exchange are shown in Fig. 2(b). These bands are quite similar to the TiS_2 bands except that the direct energy gap at p has decreased from 0.145 to 0.086 Ry. This

reduction is in agreement with the semiempirical band-model calculation.

In order to make comparisons with the optical experiments, the joint-density-of-states curve of

TABLE I. Comparison of eigenvalues of three band models of TiS_2 at Γ . Energy in Ry.

	This work	Ref. 11	Ref. 12
d bandwidth	0.105	0.140	0.105
p - d gap	0.145	0.140	0.076
p bandwidth	0.371	0.320	0.210
$4s \rightarrow \Gamma_3^+$	0.271	0.320	0.210

TiS_2 has been calculated in a model which ignores the transition matrix elements. The result is plotted as Fig. 3(a). The curve shown has been obtained by sampling 190 000 uniformly distributed points in the Brillouin zone (BZ); for a sampling of only 50 000 points in the BZ the curve is generally unaltered. The main features of the joint-density-of-states curve, which can be compared to the transmission spectra, are the shoulders at 0.80, 1.60, and 2.15 eV, the relative maxima at 2.42 and 3.26 eV, and the valley at 2.55 eV. The features of the calculated curve are measured relative to a reduced band gap E'_{gap} , which is determined by fitting the calculated band gap to the optical band gap.⁷ Predictions of the present calculations for optical transitions are compared with the experimental data in Table II.

The above six features of the calculated curve correspond to the shoulders at 1.04, 1.64, and 2.01 eV, the relative maxima at 2.29 and 3.37 eV and the valley at 3.0 eV of the transmission spec-

TABLE II. Features in spectra of TiS_2 .

Direct transition	TiS_2 calculated energy (eV)	Observed energy (eV) and features	
$\Gamma_2^- \rightarrow \Gamma_3^+$			
$\Gamma_2^- \rightarrow \Gamma_1^+$	0.8	1.04	Shoulder
$M_2^- \rightarrow M_1^+$	1.60	1.64	Shoulder
$\Gamma_3^- \rightarrow \Gamma_3^+$	2.15	2.01	Shoulder
$M_2^- \rightarrow M_1^+$			
$M_2^- \rightarrow M_1^+$	2.42	2.29	Peak
$K_2 \rightarrow K_3$	3.26	3.37	Peak
$M_1^- \rightarrow M_2^+$			
$K_1 \rightarrow K_3$	5.70	...	Peak

tra. The over-all comparison is fair except for a relative shift of the valley in the region between 2.5 and 2.7 eV. The transmission spectra were measured up to energies of 3.5 eV, so no comparison can be made at higher energies with this calculation. However, we have found additional structure at higher energies: a minima at 4.2 eV, a maxima located at 5.7 eV and a shoulder at 3.5 eV.

The joint density of states (JDS) of TiSe_2 shown in Fig. 3(b) has been calculated by sampling the

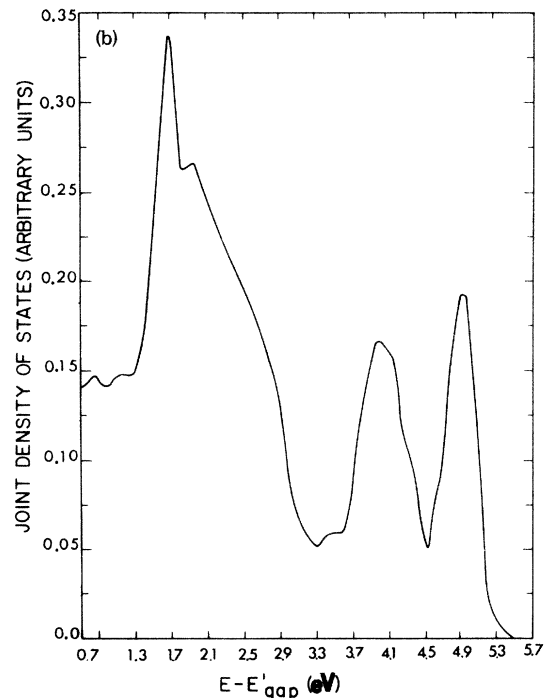
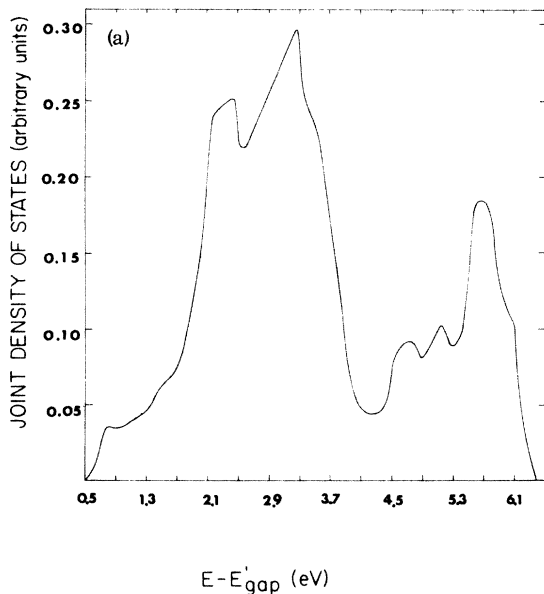
FIG. 3. (a) Joint density of states of TiS_2 . (b) Joint density of states of TiSe_2 .

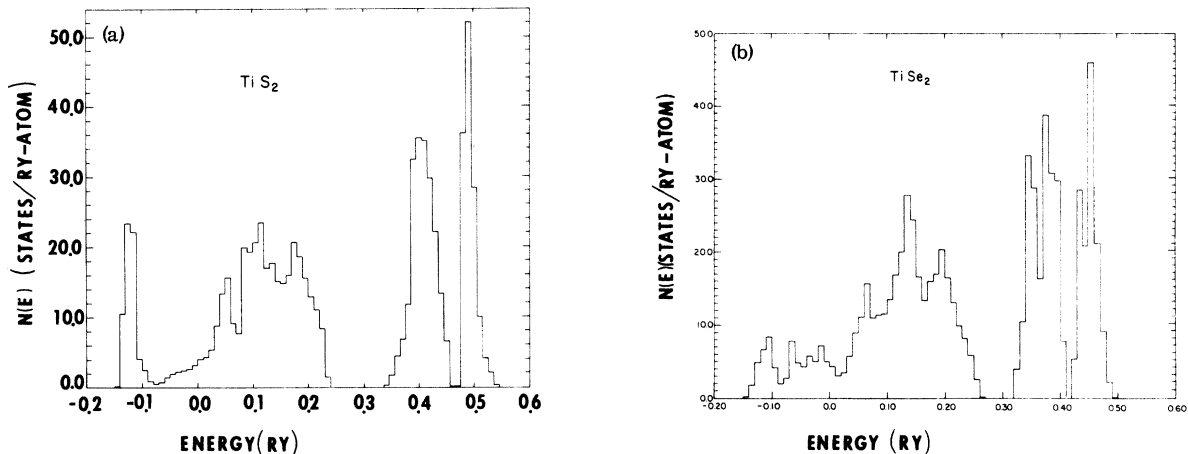
TABLE III. Features in spectra of TiSe_2 .

Direct transition	TiSe_2 calculated energy (eV)	Observed energy (eV) and features	
$\Gamma_3^- \rightarrow \Gamma_3^+$			
$\Gamma_3^- \rightarrow \Gamma_1^+$	0.83	1.34	Shoulder
$\Gamma_2^- \rightarrow \Gamma_3^+$	1.09	1.58	Shoulder
$L_1^- \rightarrow L_1^+$	1.67	1.63	Peak
Along U	1.89	1.92	Shoulder
	...	2.70	Shoulder
$A_3^+ \rightarrow A_1^+$			
$M_2^- \rightarrow M_1^+$	2.90	2.94	Shoulder
$M_2^- \rightarrow M_2^+$	3.35	3.18	Shoulder
$L_2^- \rightarrow L_2^+$			
$K_2^- \rightarrow K_3^+$	3.95	3.46	Broad peak
$A_2^- \rightarrow A_3^+$			
$L_2^- \rightarrow L_1^+$			
$L_2^- \rightarrow L_2^+$			
$L_1^- \rightarrow L_1^+$			
$K_2^- \rightarrow K_3^+$	4.48	...	Peak
$M_2^- \rightarrow M_1^+$			
$M_1^- \rightarrow M_2^+$			
$M_1^- \rightarrow M_2^+$			
$A_1^+ \rightarrow A_1^+$			
$H_2^- \rightarrow H_3^+$			

same points in the BZ as previously outlined. The main features of the JDS and the transmission spectra⁷ are outlined in Table III. It is clear that the general features of the transmission spectra are obtained for both TiS_2 and TiSe_2 . Better agreement is not to be expected because of the omission of matrix elements, the hole-state-excitation problem already mentioned and fact that since these calculations do not include muffin-tin (MT) corrections, the resulting metal d bands are narrower than if MT corrections had been included.¹⁹ This change in d bandwidths causes relative shifts in features of any resulting joint density of states.

The electronic density of states of TiS_2 and TiSe_2 , shown in Fig. 4(a) and 4(b), have been calculated from the energy eigenvalues of the KKR calculations on the same grid of points used to calculate the joint density of states just discussed. This was done in order to discuss the possible relevance of these results to the observation of a high T_c in $\text{Li}_x\text{Ti}_{1.1}\text{S}_2$ and the predictions of a microscopic model of superconductivity for this system.⁵ Figure 4 shows the expected energy separation of the density of states into several distinct regions corresponding to the chalcogen $s-p$ bands at lower energy and the Ti d bands at higher energy. A major feature of the results is the fact that the metal d bands are narrower than the $s-p$ bands of the ligands or even the p bands alone. Note also the separation of the d bands themselves into two narrow highly peaked parts also separated by a (small) gap.

As remarked in the Introduction, Phillips⁵ has called attention to the possible role of very high $dN(E_F)/dE$ values in giving rise to high values of T_c such as might be expected in the $\text{Li}_x\text{Ti}_{1.1}\text{S}_2$ system. It is interesting to note that the very high

FIG. 4. (a) Electronic density of states of TiS_2 . (b) Electronic density of states of TiSe_2 .

dN/dE seen in Fig. 4 at the low-energy side of the d bands do satisfy this condition. If one assumes some very simple mechanism (such as a rigid-band model) for the doping process involved in adding excess Ti and Li atoms to TiS_2 then 0.5–0.7 electrons (essentially all the excess valence electrons) added to the valence bands would shift E_F in Fig. 4(a) upward to between 0.374 and 0.379 Ry, which is the vicinity of the large change in the electronic density of states. While the systematics of a connection between $dN(E_F)/dE$ and the effective electron-electron interaction parameter responsible for T_c are not established, there has been a good deal of interest recently in narrow-band superconductivity. Following the strong correlation between atomic properties and T_c pointed out by Matthias,²⁰ Appel and Kohn²¹ have formulated a theory which emphasizes the importance of the intra-atomic Coulomb correlation interaction U . In par-

ticular, they stressed the effects caused by variations of U and (to a smaller extent) the electronic bandwidth. It appears possible that narrow d bands, of the type shown in Fig. 4, if occupied by electrons through some doping or alloying process, would be good candidates for high T_c behavior.

Finally, in order to help resolve the controversy whether TiS_2 is a metal or semiconductor, we have calculated the energy bands resulting from potentials generated using several different exchange approximations. In all cases, we have always found a gap between the valence band and the conduction band. It is apparent, in the light of these results, the relative good agreement with the discrete-variational-method band calculations,¹¹ and the comparison of these calculations with the transmission spectra, that there is need for a different interpretation of the "metallic" nature of TiS_2 by the x-ray⁸ and transport-property⁹ work.

†Supported by the Air Force Office of Scientific Research, the National Science Foundation, and the Atomic Energy Commission.

¹J. A. Wilson and A. D. Yoffe, *Adv. Phys.* **18**, 193 (1969).

²F. Hullinger, *Struct. Bonding* **4**, 83 (1968).

³F. R. Gamble, F. J. DiSalvo, R. A. Klemm, and T. H. Geballe, *Science* **168**, 568 (1970); F. R. Gamble, J. H. Osiecki, M. Cais, R. Phisarody, F. J. DiSalvo, and T. H. Geballe, *Science* **174**, 493 (1971); F. R. Gamble, J. H. Osiecki, and F. J. DiSalvo, *J. Chem. Phys.* **55**, 3525 (1971).

⁴H. E. Barz, A. S. Cooper, E. Corenzwit, M. Marezio, B. T. Matthias, and P. H. Schmidt, *Science* **175**, 884 (1972).

⁵J. C. Phillips, *Phys. Rev. Lett.* **28**, 1196 (1972).

⁶W. L. McMillan, *Phys. Rev.* **167**, 331 (1968).

⁷A. R. Beal, J. C. Knight, and W. Y. Liang, *J. Phys. C* **5**, 3531 (1972).

⁸D. W. Fischer, *Phys. Rev. B* **8**, 3576 (1973).

⁹A. H. Thompson, K. R. Pisharody, and R. F. Koehler, Jr., *Phys. Rev. Lett.* **29**, 163 (1972).

¹⁰J. Koringa, *Physica (Utr.)* **13**, 392 (1947); W. Kohn and N. Rostoker, *Phys. Rev.* **94**, 1111 (1954).

¹¹D. E. Ellis and A. Seth, *Int. J. Quantum Chem.* (to be published).

¹²R. B. Murray and A. D. Yoffe, *J. Phys. C* **5**, 3038 (1972).

¹³L. F. Mattheiss, *Phys. Rev.* **133**, A1399 (1964).

¹⁴J. C. Slater, *Phys. Rev.* **81**, 385 (1951).

¹⁵W. Kohn and L. J. Sham, *Phys. Rev.* **140**, A1133 (1965); R. Gaspár, *Acta Phys. Acad. Sci. Hung.* **3**, 263 (1954).

¹⁶F. S. Ham and B. Segall, *Phys. Rev.* **124**, 1786 (1961).

¹⁷H. W. Myron, Ph.D. thesis (Iowa State University, 1972) (unpublished).

¹⁸Jerry C. Shaw, J. B. Ketterson, and L. R. Windmiller, *Phys. Rev. B* **5**, 3894 (1972).

¹⁹L. F. Mattheiss, *Phys. Rev.* **181**, 987 (1969); L. F. Mattheiss, *Phys. Rev. Lett.* **30**, 784 (1973).

²⁰B. Matthias, *Phys. Rev.* **97**, 74 (1955).

²¹J. Appel and W. Kohn, *Phys. Rev. B* **4**, 2162 (1971); *Phys. Rev. B* **5**, 1823 (1972).